Journal of Hazardous Materials 165 (2009) 63–70

Contents lists available at ScienceDirect

Journal of Hazardous Materials

journal homepage: www.elsevier.com/locate/jhazmat

Removal of lead ions by Unye (Turkey) bentonite in iron and magnesium oxide-coated forms

Erdal Eren*

Ahi Evran University, Faculty of Arts and Science, Department of Chemistry, 40100 Kırsehir, Turkey

ARTICLE INFO

Article history:
Received 2 June 2008
Received in revised form 23 August 2008
Accepted 19 September 2008
Available online 26 September 2008

Keywords:
Bentonite
Adsorption
Thermodynamic
Clay
Lead

ABSTRACT

This paper presents the adsorption of Pb(II) from aqueous solution onto Unye (Turkey) bentonite in raw (RB), iron oxide-coated (ICB) and magnesium oxide-coated (MCB) forms. Adsorption of Pb(II) by samples was investigated as a function of the initial Pb(II) concentration, solution pH, ionic strength, temperature and inorganic ligand effect (Cl^-). Changes in the surface and structure were characterized by means of XRD and N_2 gas adsorption data. The Langmuir monolayer adsorption capacities of RB, ICB and MCB in 0.1 M KNO_3 solution were estimated as 16.70, 22.20 and 31.86 mg/g, respectively. The spontaneity of the adsorption process is established by decrease in ΔG which varied from −21.60 to −28.60 kJ/mol (RB), −21.74 to −32.22 kJ/mol (ICB) and −26.27 to −33.11 (MCB) in temperature range 303–338 K.

1. Introduction

The contamination of water by heavy metals through the discharge of industrial wastewater is a worldwide environmental problem. Heavy metals may come from various industrial sources such as electroplating, metal finishing, metallurgy, chemical manufacturing, mining and battery manufacturing. Removal of heavy metal ions from wastewater in an effective manner has become an important issue today. The heavy metal removal methods are chemical precipitation, membrane filtration, ion exchange and adsorption [1]. Adsorption process provides an attractive alternative treatment to other removal techniques because it is more economical and readily available. A lot of non-conventional, low-cost and easily obtainable adsorbents have been tested for heavy metal removal such as clay minerals [2–5], biomaterials [6–9] and industrial solid wastes [10–13]. Those studies indicated that the adsorption capacity of most low-cost materials is much less effective than that of commercial adsorbents.

Bentonite is natural clay that is found in many places of the world. Any clay of volcanic origin that contains montmorillonite is referred to bentonite. It belongs to the 2:1 clay family, the basic structural unit of which is composed of two tetrahedrally coordinated sheets of silicon ions surrounding a sandwiched octahedrally coordinated sheet of aluminum ions. The isomorphous substitution of Al^{3+} for Si^{4+} in the tetrahedral layer and Mg^{2+} or Fe^{3+} for Al^{3+} in the octahedral layer results in a net negative surface charge on the clay [14]. Also, montmorillonite have amphoteric pH-dependent surfaces, high exchange capacity and different modes of aggregation [14,15]. Amphoteric surfaces of the montmorillonite provide suitable adsorption sites for cations. This character of montmorillonite makes it a potential adsorbent for adsorption heavy metal from aqueous solutions.

The heavy metal adsorption onto iron, manganese oxide-coated adsorbents have received wider attention than that of magnesium oxide-coated adsorbents [15–21]. In the present work, a cheap, readily available and effective adsorbent material has identified bentonite as a potentially attractive adsorbent for the treatment of Pb(II) contaminated aqueous solutions after coating with iron and magnesium oxides. Since there is a huge deposit of bentonite, there is a great potential for its utilization in wastewater treatment. The main objective of this study was to investigate the feasibility of using iron and magnesium oxides coated bentonite for the maximum removal of Pb(II) ions from aqueous solutions.

2. Materials and methods

2.1. Materials

All reagents used were of analytical purity. Synthetic solutions were prepared from concentrated stock solutions (Merck). A stock solution of Pb(II) was prepared by dissolving required amount of $Pb(NO_3)_2$ (Merck) in double distilled water. HNO_3 and NaOH were

* Tel.: +90 386 211 45 00; fax: +90 386 211 45 25.
E-mail address: eeren@ahievran.edu.tr.

0304-3894/$ – see front matter © 2008 Elsevier B.V. All rights reserved.
doi:10.1016/j.jhazmat.2008.09.066

Nomenclature

C_e	equilibrium concentration of the adsorbate in the solution (mg/l);
ICB	iron oxide-coated bentonite
IS	ionic strength
K_L	constant that represents the energy or net enthalpy of adsorption (l/mg);
K_F	Freundlich constant indicative of the adsorption capacity of the adsorbent (mg/g);
m	mass of adsorbent (g/l);
MCB	magnesium oxide-coated bentonite
n	experimental constant indicative of the adsorption intensity of the adsorbent.
q_e	amount of adsorbate removed from aqueous solution at equilibrium (mg/g);
q_m	mass of adsorbed solute completely required to saturate a unit mass of adsorbent (mg/g);
RB	raw bentonite

obtained from Merck and used for pH value adjustment. Other agents used, such as NaCl, $Fe(NO_3)_3$, $Mg(NO_3)_2$ and KNO_3 were all of analytical grade and all solutions were prepared with double distilled water.

2.1.1. Preparation of RB

The RB sample (from Unye, Turkey) was ground and washed in deionized water several times at a 1:10 bentonite/water ratio. The mixture was stirred for 3 h and then kept standing overnight, followed by separation, washing and drying at 60 °C.

RB had a mineral composition of 76% montmorillonite, 8% quartz, 12% dolomite and 4% other minerals. Whiteness was found to be 85%. RB was composed of 62.70% SiO_2, 20.10% Al_2O_3, 2.16% Fe_2O_3, 2.29%CaO, 3.64% MgO, 0.27% Na_2O, 2.53% K_2O, 0.21% TiO_2 and 0.02% P_2O_5. The ignition loss of the RB at 1273 K was also found to be 6.1%. The cation exchange capacity (CEC), determined with triethanolamine-buffered $BaCl_2$ solution (c = 0.1 M) followed by a reexchange with aqueous $MgCl_2$ solution (c = 0.1 M), is of 0.65 mmol/g [22]. The total pore volume value is 0.07 cm^3/g, the micropores contribute to 11.42% of total pore volume. The average pore diameter is 8.11 nm.

2.1.2. Preparation of ICB

The system was prepared by mixing 20.0 g of RB, 100 ml of freshly prepared 1 M $Fe(NO_3)_3 \cdot 9H_2O$ solution, and 180 ml of 2 M NaOH solution in a 2 l polyethylene flask. The addition of NaOH solution was rapid and with stirring. The suspension was diluted to 2 l with twice distilled water and was held in a pyrex glass beaker flask at 80 °C for 48 h. After the appropriate period the precipitate was centrifuged, washed (until free of NO_3^- ions) and finally dried [23,24].

2.1.3. Preparation of MCB

Magnesium nitrate and sodium hydroxide were mainly used in the coating of RB to enhance the adsorption capacity of RB. Twenty grams of RB were immersed in sufficient 2 M sodium hydroxide and temperature of the reaction mixture was maintained at 90 °C for 4 h. The base activated RB was dispersed into 150 ml of 0.1 M $Mg(NO_3)_2$ aqueous solution. Three hundred microliters of 0.1 M NaOH aqueous solution was added slowly with a drop rate 1 ml/h. The titration was carried out under nitrogen flow throughout the procedure to minimize unexpected reactions, e.g. formation of carbonate salts. The obtained powder was rinsed with 0.01 M HCl aqueous solution to remove the excess $Mg(OH)_2$ precipitated on the outer surface of the clay and further washed with deionized water. Then, this sample was heated for 4 h in air at 700 K. The thermal treatment of mixed solids in air at 700 K leads to the formation of MgO [25,26].

The mineralogical compositions of the RB and MCB samples were determined from the X-ray diffraction (XRD) patterns of the products taken on a Rigaku 2000 automated diffractometer using Ni filtered Cu Kα radiation. XRD analysis of the bentonite was performed using the three-principal lines. The surface areas were calculated by the Brunauer–Emmett–Teller (BET) method. The BET surface area (S_{BET}), external surface area (including only mesopores $S_{ext.}$), micropores surface area ($S_{mic.}$), total pore volume (V_t) and average pore diameter (D_p) results obtained by applying the BET equation to N_2 adsorption at 77 K and Barret–Joymer–Halenda (BJH) equation to N_2 adsorption at 77 K.

2.2. Adsorption dependence on Pb(II) concentration

The adsorption of Pb(II) by bentonite samples was performed by a batch equilibrium technique at room temperature. Briefly, 0.050 g of bentonite sample and 20 ml of $Pb(NO_3)_2$ solution were added in 50 ml polyethylene test tubes. Ionic strength controlled at 0.1 M KNO_3 and the pH of the system was maintained at 6.0. The initial Pb(II) concentrations varied from 0.01 to 1.0 mM. A 24-h contacting period was found to be sufficient to achieve equilibrium. The samples were allowed to equilibrate for 24 h, centrifuged at 4500 × g for 20 min and then decanted. All the measurements were made in duplicate and the average values were reported. An experiment without adsorbent was performed to test possible adsorption and/or precipitation of Pb(II) onto the test tube walls. Preliminary experiments showed that Pb(II) losses due to the adsorption onto the test tubes were negligible. Adsorbed Pb(II) was calculated from the difference between the Pb(II) initially added to the system and that remaining in the solution after equilibration by a Unicam 929 model flame atomic absorption spectrophotometer, Pb(II): lamp current 10 mA, wavelength 217.1 nm, slit width 0.5 nm, optimum working range 2–10.0 μg/ml; flame type air/acetylene, fuel flow rate 1.2 l/s. The dilutions induced by the pH controls were considered while computing the amount of Pb(II) adsorbed.

2.3. Effect of ionic strength, pH, inorganic ligand and temperature

Adsorption experiments were carried out in polyethylene test tubes at 23 ± 2 °C by using the batch technique. The reaction mixture consisted of a total 50 ml containing 2 g/l adsorbent and the desired concentration of Pb(II) ions. A solution of 1.0 mM Pb(II) was prepared from $Pb(NO_3)_2$ by dissolving in deionized water. The stock was diluted to prepare a working solution of 0.05 mM Pb(II). The background electrolyte solutions were 0.01, 0.05, and 0.1 M KNO_3. Solution pH was adjusted with 0.1 M HNO_3 or 0.1 M NaOH, such that the equilibrium solutions had pH values ranging from 3.0 to 6.5. Preliminary kinetic studies indicated that Pb(II) adsorption was characterized by a rapid initial adsorption (within 1 h) followed by a much slower, continuous uptake. A 24 h contacting period was found to be sufficient to achieve equilibrium. The separation of the liquid from the solid phase was achieved by centrifugation at 4500 rpm for 20 min. Pb(II) adsorption in the presence of inorganic ligands was performed by equilibrating 0.05 g of bentonite sample in 20 ml of 0.25 M KNO_3 background electrolyte, 10 ml of Pb(II) working solution, and 20 ml of NaCl working solution (achieving 0.01 M ligand) in 50 ml polyethylene test tubes. These experiments were performed in duplicate. For thermodynamic studies, the temperature was varied from 303 to 338 K at a constant pH of 6.0. Two gram per liter of MCB with 10.3 mg/l Pb (II) solutions was employed for these experiments.

2.4. Theoretical background

The adsorption capacity of Pb(II) ions adsorbed per gram adsorbent (mg/g) was calculated using the equation:

$$q_e = \frac{(C_0 - C_e)V}{m} \quad (1)$$

The adsorption percentage of Pb(II) ions was calculated by the difference of initial and final concentration using the equation expressed as follows:

$$R = \frac{C_0 - C_e}{C_0} \times 100 \quad (2)$$

where q_e is the equilibrium concentration of Pb(II) on the adsorbent (mg/g), C_0 the initial concentration of the Pb(II) solution (mg/l), C_e the equilibrium concentration of the Pb(II) solution (mg/l), m the mass of adsorbent (g), V the volume of Pb(II) solution (l), and R is the retention of Pb(II) in % of the added amount.

The analysis of the isotherm data by fitting them to different isotherm models is an important step to find the suitable model that can be used for design purpose. There are several isotherm equations available for analyzing experimental adsorption equilibrium data. In this study, the equilibrium experimental data for adsorbed Pb(II) on bentonite sample were analyzed using the Langmuir, Freundlich and Dubinin–Radushkevich (D–R) isotherm models. These isotherms are as follows:

(a) Langmuir isotherm model [27]:

$$\frac{C_e}{q_e} = \frac{C_e}{q_m} + \frac{1}{K_L q_m} \quad (3)$$

where C_e is equilibrium concentration of Pb(II) (mg/l) and q_e is the amount of the Pb(II) adsorbed (mg) by per unit of bentonite (g). q_m and K_L are the Langmuir constants related to the adsorption capacity (mg/g) and the equilibrium constant (l/mg), respectively.

(b) Freundlich isotherm model [28]:

$$\log\ q_e = \log K_F + \left(\frac{1}{n}\right) \log C_e \quad (4)$$

where K_F and n are Freundlich constants related to adsorption capacity and adsorption intensity, respectively.

(c) D–R isotherm model [1,29–32]:

$$\ln\ q_e = \ln q_m - \beta\varepsilon^2 \quad (5)$$

where β is the activity coefficient related to mean adsorption energy (mol^2/J^2) and ε is the Polanyi potential ($\varepsilon = RT\ln(1 + (1/C_e))$). The D–R isotherm is applied to the data obtained from the empirical studies. The mean adsorption energy, E (kJ/mol) is as follows:

$$E = \frac{1}{\sqrt{-2\beta}} \quad (6)$$

This adsorption potential is independent of the temperature, but it varies depending on the nature of adsorbent and adsorbate.

Using the following equations, the thermodynamic parameters of the adsorption process can be determined from the experimental data:

$$\ln\ K_d = \frac{\Delta S}{R} - \frac{\Delta H}{RT} \quad (7)$$

$$\Delta G = \Delta H - T\Delta S \quad (8)$$

$$K_d = \frac{q_e}{C_e} \quad (9)$$

where K_d is the distribution coefficient for the adsorption, ΔS, ΔH and ΔG are the changes of entropy, enthalpy and the Gibbs energy, q_e is the equilibrium concentration of Pb(II) on the adsorbent (mg/g), T (K) is the temperature, R (J mol^{-1} K^{-1}) is the gas constant.

3. Results and discussion

3.1. Material characterization

The XRD patterns of RB, ICB and MCB samples were presented in Fig. 1. For the XRD pattern of RB, one reflection was observed in the region $2^\circ < 2\theta < 8^\circ$ (Fig. 1a). This corresponds to the 5.76 (2θ) value from which the interlamellar distance was found to be 15.33 Å. The position of d_{001} peak of MCB sample shifted from 15.33 to 14.31 Å (Fig. 1b) which was accompanied by a intensity decrease from 100 to 9.4% (Table 1). The XRD results also show that Mg oxide-coating process has caused structural changes in the bentonite sample. Metal oxide-coating process of the RB has affected mainly the 0 0 1 reflection; the intensities of the 0 0 1 and 0 0 6 reflections has been reduced, while the intensities of the 0 2 0 and 0 6 0 reflections has been increased significantly by the coating process (Table 1).

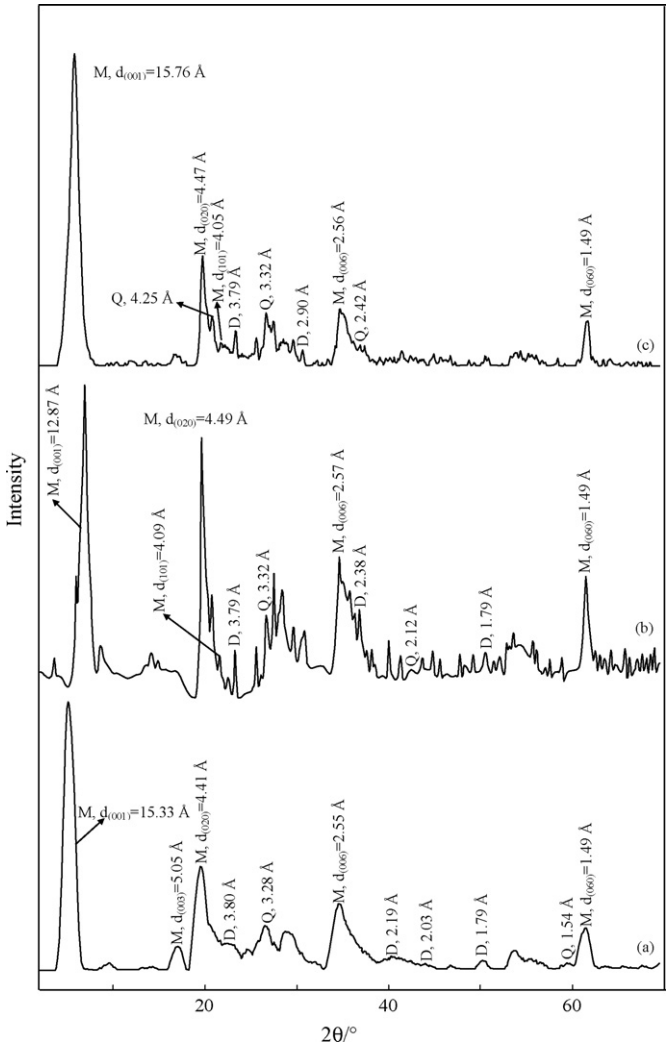

Fig. 1. The XRD patterns of the RB (a), ICB (b) and MCB (c) samples (M: montmorillonite, D: Dolomite, Q: quartz).

Table 1
d-Spacing and intensity values of reflections for bentonite samples.

Reflection	RB		ICB		MCB	
	d (Å)	I/I_0	*d* (Å)	I/I_0	*d* (Å)	I/I_0
d_{001}	15.33	100	12.87	100	14.31	9.4
d_{003}	5.05	8	–	–	–	–
d_{020}	4.42	34	4.49	92	4.45	100
d_{101}	–	–	4.09	7	4.05	5.9
d_{006}	2.55	21	2.57	32	2.55	13
d_{060}	1.49	13	1.49	35	1.49	41

Metal oxide-coating process of the RB yielded d_{101} reflection at 4.05 Å ($2\theta = 21.68$), which is absent in the RB. Appearance of new reflection indicates the formation of expansible phases and interlamellar expansion [33]. The d_{003} reflection of RB at 5.05 Å ($2\theta = 17.52$) disappeared after oxide-coating processes. The formation of a new structure was illustrated by the peak appearing at lower <6.17° in the XRD pattern of the MCB. The new peaks situated at lower 2θ value (<6.17°) were likely to appear because of agglomeration of the MCB sheets [34]. MCB sample displays an increase of the background in the interval between 20° and 30°.

The data in Table 2 indicate the surface areas, pore volumes and average pore diameter for RB and oxide-coated samples. The pore structure evolution of RB after iron oxide-coating process is different from that of the magnesium oxide-coating process. The results indicated that the micropores and parts of mesopores on bentonite were occupied with magnesium oxide. Obviously, the iron oxide-coating process leads to a simultaneous micropore widening and an increase in the micropore volume. This increase in the micropore size and the micropore volume might be due to the insertion of iron oxide between the clay sheets during the coating process, which could create a larger interlayer space and, consequently, head to larger micropore diameters and micropore spaces.

3.2. Adsorption isotherms and parameters

The equilibrium data for Pb(II) adsorption on bentonite samples were fitted to Langmuir equation (Eq. (3)): an equilibrium model able to identify chemical mechanism involved. Linear plots of C_e/q_e versus C_e (Fig. 2) were employed to determine the value of q_m (mg/g) and K_L (l/mg). The data obtained with the correlation coefficients (R^2) was listed in Table 3. The Langmuir monolayer adsorption capacities of RB, ICB and MCB in 0.1 M KNO_3 solution were estimated as 16.70, 22.20 and 31.86 mg/g, respectively (Table 3). As given in Table 3, the equilibrium constant values for RB, ICB and MCB were found to be 1.30, 0.87 and 3.79, respectively.

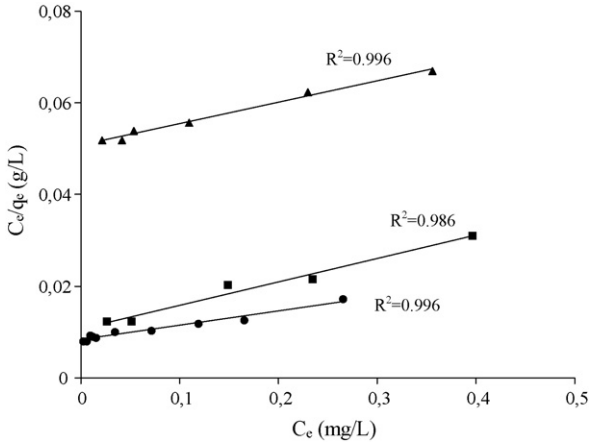

Fig. 2. Langmuir isotherm plot for the adsorption of Pb(II) onto bentonite samples. $T = 295$ K, initial pH 6.0, $m = 2$ g/l, squares, RB; triangles, ICB; circles, MCB.

The monolayer adsorption capacities of the adsorbents for the removal of Pb(II) have been compared with those of other adsorbents reported in literature and the values of monolayer adsorption capacities have been presented in Table 4. The experimental data of the present investigation are comparable with the reported values [21,24,35–47]. Zhu et al. [35] reported that Langmuir adsorption capacity for Pb(II) on bentonite has been shown to be 78.82 mg/g. The uptake of Pb(II) on MX-80 bentonite has Langmuir monolayer capacity $q_m = 68.58$ mg/g [36]. Bhattacharyya and Gupta [37] have reported a Langmuir monolayer capacity, q_m, of 33 mg/g at for Pb(II) adsorption onto montmorillonite. Adsorption of Pb(II) on clinoptilolite follows the Langmuir isotherm model with an adsorption capacity of 80.933 mg/g [38]. The uptake of Pb(II) on natural sorbent has Langmuir monolayer capacity $q_m = 66.24$ mg/g [39]. Ozer [40] reported that the Langmuir adsorption capacity for Pb(II) on sulphuric acid-treated wheat bran was found as 55.56 mg/g. Sari et al. [41] reported that the Langmuir adsorption capacity for Pb(II) on Turkish kaolinite was found as 31.75 mg/g. Comparison of maximum experimental adsorption capacities of Pb(II) for metal oxide-coated adsorbents were also given in Table 4 [21,24,44–47]. Maximum adsorption capacity of Pb(II) for the metal oxide-coated samples was approximately two to three times higher than that of the raw material. Lai and Chen [24] reported that the Langmuir adsorption capacity for Pb(II) on iron-coated sand was found as 1.211 mg/g. Langmuir adsorption capacity for Pb (II) adsorption on Al_2O_3-supported iron oxide has been shown to be 28.98 mg/g by Huang et al. [45]. The Pb(II) adsorption capacities of diatomite

Table 2
Porous structure parameters of the raw and metal oxide-coated bentonite samples.

Sample	S_{BET} (m^2/g)	$S_{ext.}$[a] (m^2/g)	$S_{mic.}$ (m^2/g)	V_t (cm^3/g)	$V_{mic.}$ (cm^3/g)	V_{meso} (cm^3/g)	D_p[b] (nm)
RB	57	19	38	0.084	0.010	0.074	5.72
ICB	63	36	27	0.084	0.013	0.067	5.30
MCB	30	10	20	0.065	0.005	0.060	7.82

[a] $S_{ext} = S_{meso}$.
[b] $4\,V/A$ by BET.

Table 3
Langmuir, Freundlich and D–R isotherm parameters for the adsorption of Pb(II) onto bentonite samples.

Sample	Langmuir isotherm constants			Freundlich isotherm constants			D–R isotherm constants		
	q_m (mg/g)	K_L (l/mg)	R^2	*n*	K_F ((mg/g) (l/mg)$^{1/n}$)	R^2	q_m (mg/g)	*E* (kJ/mol)	R^2
RB	16.70	1.30	0.986	14.30	12.86	0.942	8.46	2.98	0.971
ICB	22.20	0.87	0.996	1.14	12.77	0.978	5.43	0.73	0.977
MCB	31.86	3.79	0.996	1.16	59.24	0.965	7.57	5.32	0.991

Table 4
Adsorption results of Pb(II) ions from the literature by various adsorbents.

Adsorbent	Adsorption capacity (mg/g)	Ref. no.
Bentonite (298 K)	78.82	[35]
Montmorillonite	31.1	[36]
Montmorillonite (303 K, pH 5.7)	33	[37]
Clinoptilolite (295 K, pH 4.5)	80.933	[38]
Natural sorbent (298 K, pH 4.5, 24 h)	66.24	[30]
Acid-treated wheat bran (298 K, pH 6, 2 h)	55.56	[40]
Turkish kaolinite (295 K, pH 5)	31.75	[41]
Sand	≈0	[42]
Al_2O_3	17.5	[43]
Iron-coated sand (IS = 0.1 M $NaNO_3$, pH 6)	1.211	[24]
Manganese oxide coated sand (303 K)	1.34	[44]
Al_2O_3-supported iron oxide (300 K, pH 5)	28.98	[45]
Diatomite (pH 5, 24 h)	24.0	[46]
Mn-diatomite (pH 5, 24 h)	99.0	[46]
Mn oxide-coated carbon nanotube (pH 5)	78.74	[47]
Carbon nanotube (pH 5)	≈26.24	[47]
RB (IS = 0)	64.29	[21]
RB (IS = 0.1 M KNO_3)	16.70	[21]
Mn oxide-coated RB (IS = 0)		[21]
Mn oxide-coated (IS = 0.1 M KNO_3)		[21]
ICB (IS = 0.1 M KNO_3)	22.20	In this study
MCB (IS = 0.1 M KNO_3)	31.86	In this study

IS: Ionic strength (controlled by KNO_3).

and Mn-diatomite were determined as 24 and 99 mg/g, respectively [46]. In another study, Wang et al. [47] studied with Mn oxide-coated carbon nanotube, for Pb(II) removal from aqueous solution. They reported that the carbon nanotube adsorbed Pb(II) with the adsorption capability of ≈26.24 mg/g. The capacity of the Mn oxide-coated carbon nanotube increased to 78.74 mg/g. From these observations, it is appeared that the surface properties of raw bentonite could be improved upon coating of metal oxide as previously reported by other researchers [21,24,44–47].

The equilibrium data also fitted to Freundlich equation (Eq. (4)), a fairly satisfactory empirical isotherm can be used for non-ideal adsorption. The Freundlich isotherm constants K_F and n are constants incorporating all factors affecting the adsorption process such as of adsorption capacity and intensity of adsorption. The constants K_F and n were calculated from Eq. (4) and Freundlich plots (Fig. 3). The values for Freundlich constants and correlation coefficients (R^2) for the different adsorbents used during the study are also presented in Table 3. Freundlich parameters (K_F and n) indicate whether the nature of adsorption is either favorable or unfavorable. The intercept is an indicator of adsorption capacity and the slope is an indicator of adsorption intensity. A relatively slight slope $n \ll 1$ indicates that adsorption intensity is favorable over the entire range of concentrations studied, while a steep slope ($n > 1$) means that adsorption intensity is favorable at high concentrations but much less at lower concentrations. In the adsorption systems, n value is >1 which indicates that adsorption intensity is favorable over the entire range of concentrations studied. The K_F value of the Freundlich equation (Table 3) also indicates that MCB has a very high adsorption capacity for lead ions in aqueous solutions.

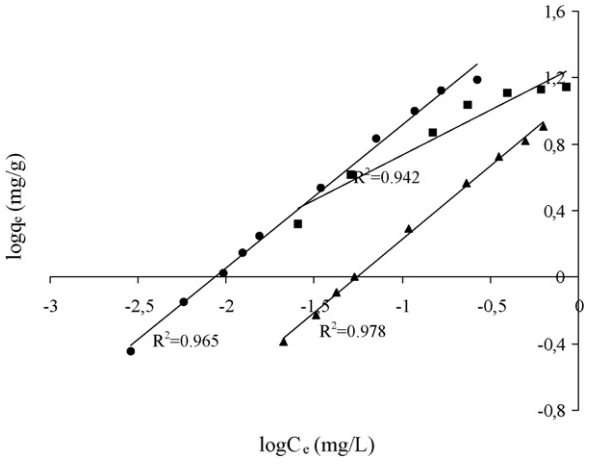

Fig. 3. Freundlich isotherm plot for adsorption of Pb(II) onto bentonite samples. T = 295 K, initial pH 6.0, m = 2 g/l, squares, RB; triangles, ICB; circles, MCB.

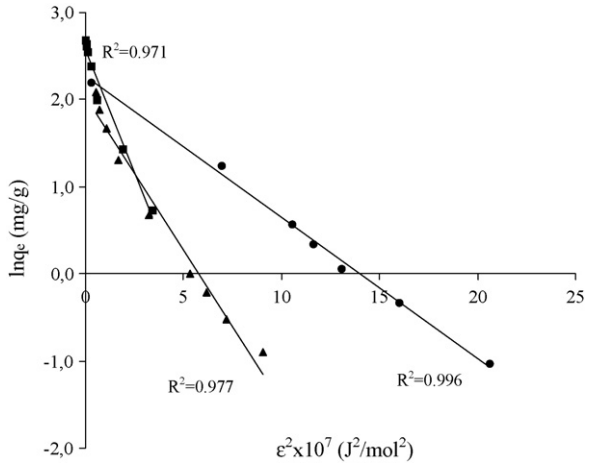

Fig. 4. D–R isotherm plot for adsorption of Pb(II) onto bentonite samples. T = 295 K, initial pH 6.0, m = 2 g/l, squares, RB; triangles, ICB; circles, MCB.

A plot of $\ln q_e$ against ε^2 is given in Fig. 4. D–R isotherm constants, q_m, for RB, ICB and MCB in 0.1 M KNO_3 solution were found to be 8.46, 5.43 and 7.57 mg/g, respectively (Table 3). The difference of q_m derived from the Langmuir and D–R models is large. The difference may be attributed to the different definition of q_m in the two models. In Langmuir model, q_m represents the maximum adsorption of metal ions at monolayer coverage, whereas it represents the maximum adsorption of metal ions at the total specific micropore volume of the adsorbent in D–R model. Thereby, the value of q_m derived from Langmuir model is higher than that derived from D–R model. The differences are also reported in previous studies [29,31]. The magnitude of E is used for estimating the type of adsorption mechanism. If the E value is between 8 and 16 kJ/mol, the adsorption process follows by chemical adsorption and if $E < 8$ kJ/mol, the adsorption process is of a physical nature [29–33]. The calculated values of E are 2.98, 0.73 and 5.32 kJ/mol for RB, ICB and MCB, respectively, and they are in the range of values for physical adsorption reactions. The similar results for the adsorption of Cr(III), Pb(II) and Zn(II) were reported by earlier workers [29,33].

3.3. Effect of ionic strength, pH and inorganic ligand

The adsorption of Pb(II) onto the bentonite samples as a function of ionic strength and pH was shown in Fig. 5a–c. The three bentonite samples showed an identical behaviour of increased uptake of Pb(II) per unit mass with gradually increasing pH, and the shape of curves dependent on the bentonite surfaces. As shown in Fig. 5a, Pb(II) adsorption by the RB sample decreased when pH decreased. This result suggests that the adsorptive decrease was caused by the competition for exchange sites between H^+ and Pb(II) cations. At low pH there is also a decrease in Pb(II) adsorption with increasing ionic strength. The adsorption curves of ICB have a similar shape as that of RB sample (Fig. 5b). The adsorption curve for this sample is characterized by two distinct adsorption edges. For example, the

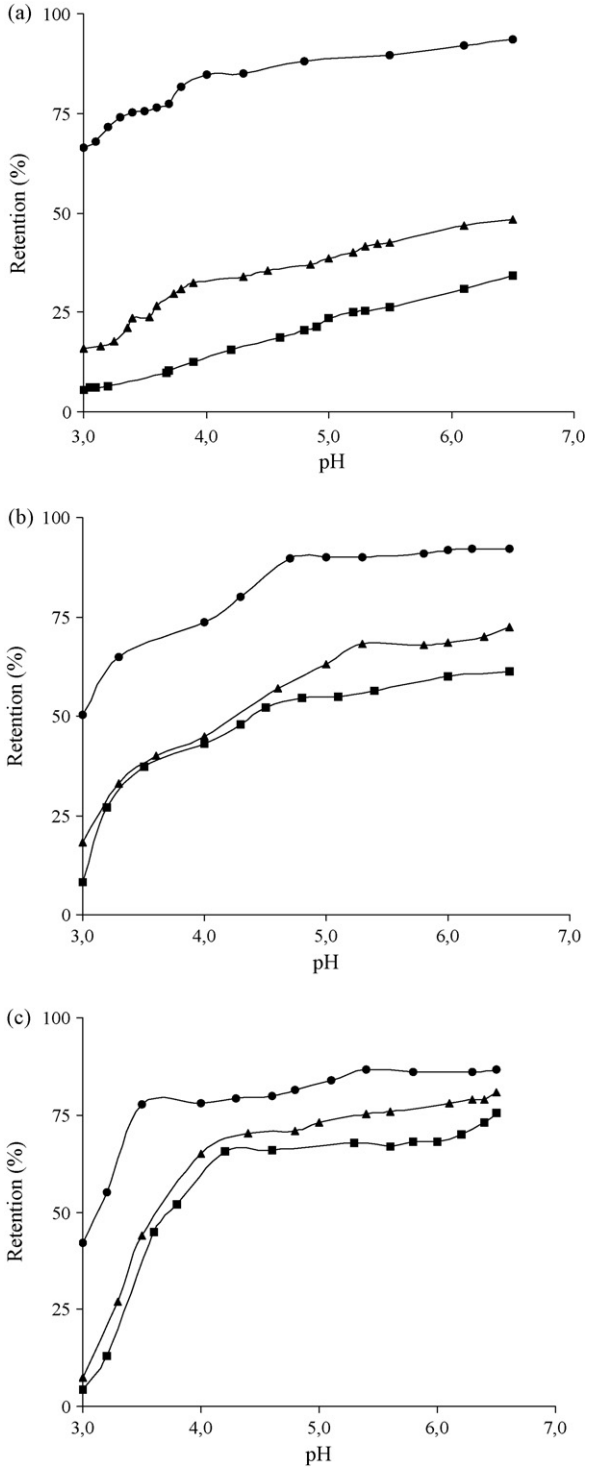

Fig. 5. (a) Adsorption of Pb(II) (10.3 mg/l) by RB (2 g/l) as function of pH and ionic strength (IS) (IS controlled by KNO_3), squares, 0.1 M; triangles, 0.05 M; circles, 0.01 M. (b) Adsorption of Pb(II) (10.3 mg/l) by ICB (2 g/l) as function of pH and ionic strength (IS controlled by KNO_3), squares, 0.1 M; triangles, 0.05 M; circles, 0.01 M. (c) Adsorption of Pb(II) (10.3 mg/l) by MCB (2 g/l) as function of pH and ionic strength (IS controlled by KNO_3), squares, 0.1 M; triangles, 0.05 M; circles, 0.01 M.

first stage of adsorption edge commenced about 8% Pb(II) adsorption at pH ~ 3.0 and ended at pH ~ 4.0, at which about 43% of the total Pb(II) had been adsorbed in the presence of 0.1 M KNO_3. The second stage started at pH 4.0 and continued up to pH 5.5 where about 61% of the total Pb(II) was adsorbed.

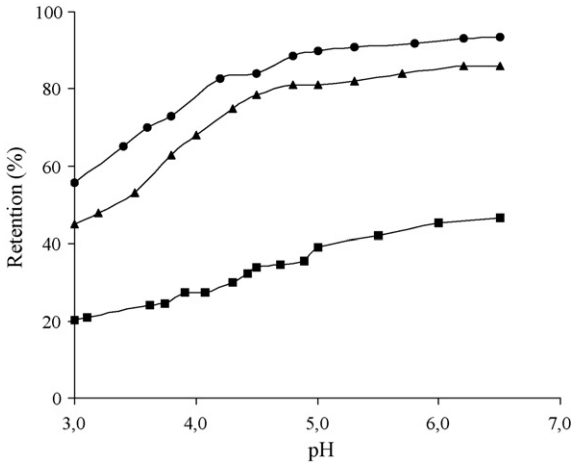

Fig. 6. Adsorption of Pb(II) (10.3 mg/l) by bentonite samples (2 g/l) as function of pH and in the presence of Cl^- [IS is 0.1 M (KNO_3)], squares, RB; triangles, ICB; circles, MCB.

The adsorption of Pb(II) onto MCB sample as a function of ionic strength and pH was shown in Fig. 5c. Increasing the ionic strength from 0.01 to 0.1 led to a significant decrease in the Pb(II) adsorption. The adsorption curves of ICB have a different shape from that of RB sample (Fig. 5c). The curves shifted to a higher pH by about pH 0.7 unit when the concentration of the background electrolyte of KNO_3 increased from 0.01 to 0.1 M. The adsorption curves for MCB are characterized by one distinct adsorption edge. For example, in the presence of 0.1 M KNO_3, the adsorption edge commenced about 4% Pb(II) adsorption at pH ~ 3.0 and ended at pH ~ 4.2, at which about 66% of the total Pb(II) had been adsorbed.

The adsorption of Pb(II) by the metal oxide-coated samples was influenced by the presence of Cl^- (Fig. 6). It is clear that aqueous speciation influences Pb(II) adsorption in the inorganic ligand system. The adsorbed Pb(II) in the presence of inorganic ligand (Cl^-) may be also attributed to a high specificity of the surfaces for Pb(II) relative to ligand. The percent Pb(II) adsorbed in the 0.01 M Cl^- systems at pH 6.5 are 86 and 94% for the ICB and MCB samples, compared to 61 and 75% at the same pH but in the absence of Cl^-. The percent Pb(II) adsorbed in the 0.1 M Cl^- system at pH 6.0 are 46% for the RB sample, compared to 34% at the same pH but in the absence of Cl^-. These results suggest that the observed Pb(II) adsorption behaviour in the bentonite suspensions is influenced by both aqueous speciation and surface ligand complexation of Pb(II) ions. The increased amount of adsorbed Pb(II) can be explained in terms of solution chemistry. Because, Pb–Cl, PbOH–Cl complexes are the dominate Pb(II) species in the presence of 0.01 M Cl^-. Thus, the specifically adsorbed ligand enhances Pb(II) retention by the surface complexation of Pb(II).

3.4. Thermodynamic studies

ΔG, ΔH° and ΔS° were evaluated for RB, ICB and MCB as −21.60 kJ/mol (at 303 K), 39 kJ/mol and 200 J/mol K, −21.74 kJ/mol (at 303 K), 69 kJ/mol and 299 J/mol K and −26.27 kJ/mol (at 303 K), 33 kJ/mol and 196 J/mol K, respectively. The negative values for the Gibbs free energy change, ΔG show that the adsorption process for the bentonite sample is spontaneous and the degree of spontaneity of the reaction increases with increasing temperature (Table 5). The increase in adsorption with temperature may be attributed to either increase in the number of active surface sites available for adsorption on the adsorbent or the desolvation of the adsorbing species and the decrease in the thickness of the boundary layer surrounding the adsorbent with temperature, so

Table 5
Thermodynamic parameters for the adsorption of Pb(II) onto bentonite samples.

Sample	ΔH (kJ/mol)	ΔS (J/mol K)	ΔG (kJ/mol)				R^2
			303	313	323	338	
RB	39	200	−21.60	−23.60	−25.60	−28.60	0.998
ICB	69	299	−21.74	−24.74	−27.73	−32.22	0.978
MCB	33	196	−26.27	−28.22	−30.18	−33.11	0.998

that the mass transfer resistance of adsorbate in the boundary layer decreases (Table 5).

The values of ΔG are less negative for the metal oxide-coated samples suggesting that the adsorption process for these materials are more spontaneous. These results suggest that the internal domains of these samples are more suitable environments for Pb(II) cations than the RB sample. Weng et al. [48] noted that ΔG° values up to 20 kJ/mol are consistent with electrostatic interaction between adsorption sites and the metal ion while ΔG° values more negative than 40 kJ/mol involve charge sharing or transfer from the adsorbent surface to the metal ion to form a coordinate bond. The values of ΔG° obtained in this work, range from −21.60 to −26.27 kJ/mol indicating that electrostatic interaction may play a significant role in the adsorption process. It may be suggested that a surface complexation reaction is the major mechanism responsible for the Pb(II) adsorption process. The negatively charged groups of Si, Al, Mg and Fe oxides on the samples favor Pb(II) adsorption. These positive values of ΔH indicate the endothermic behaviour of the adsorption reaction of Pb(II) ions and suggest that a large amount of heat is consumed to transfer the Pb(II) ions from aqueous into the solid phase. As was suggested by Nunes and Airoldi [49], the transition metal ions must give up a larger share of their hydration water before they could enter the smaller cavities. Such a release of water from the divalent cations would result in positive values of ΔS. This mechanism of the adsorption of Pb(II) ions is also supported by the positive values of ΔS, which show that Pb(II) ions are less hydrated in the bentonite layers than in the aqueous solution [50]. Also, the positive value of ΔS indicates the increased disorder in the system with changes in the hydration of the adsorbing Pb(II) cations.

Similar results are reported by Sarı et al. [29] also calculated that Gibbs free energy of Pb(II) adsorption on Celtek clay as −20.01, −19.90, −19.64 and −18.20 kJ/mol for the temperature of 293, 303, 313 and 323 K, respectively. Xu et al. [31] on adsorption of Pb(II) on MX-80 bentonite the temperature range of 291 to 328 K with ΔG increasing from −16.69 to −16.57 kJ/mol. Han et al. [44] have found that ΔH°, ΔS° and ΔG° for adsorption of Pb(II) on manganese oxide-coated sand are 18.2 kJ/mol, 117 J/kmol and −16.2 kJ/mol, respectively. Naseem and Tahir [51] have reported that ΔH°, ΔS° and ΔG° for adsorption of Pb(II) on bentonite have values of 31.74 kJ/mol, 176 J/mol K and −56.67 kJ/mol, respectively. Donat et al. [52] have found that ΔH°, ΔS° and ΔG for Pb(II) adsorption on natural bentonite were reported as 26.24 kJ/mol, 133.15 J/K mol and −38.99 kJ/mol (at 293 K), respectively.

3.5. The adsorption mechanism of Pb(II)

In view of the fact that pointed above, it is evident that metal oxide-coating process significantly enhanced the adsorption of Pb(II). It may be explained by considering the coordinative environments of lead ions and surface hydroxyl groups in hydrated surfaces. Surface hydroxyls may be present as bridging and terminal groups and metal centers may be coordinated with two or more hydroxyls. These differing configurations will give rise to terminal hydroxyl of different acidity [53]. Park et al. [54] have provided evidence about mechanism of Pb(II) adsorption on Mg/Al layered double hydroxide (LDH). XPS analysis of Pb(II)-adsorbed LDH surfaces revealed that the preferred reaction between LDH and Pb(II) is surface adsorption and precipitation. Xu et al. [55] have provided evidence about mechanism of Pb(II) adsorption on amorphous hydrous iron oxide sample. EXAFS analysis of Pb(II)-adsorbed amorphous hydrous iron oxide sample suggest that Pb(II) ions form mononuclear bidentate surface complexes on FeO_6 octahedra.

4. Conclusions

- The adsorption of Pb(II) by bentonite samples was influenced by pH, ionic strength, and the presence of Cl^-. The adsorption of Pb(II) depend upon the nature of the adsorbent surface and the species distribution of Pb(II) in solution, which mainly depends on the pH of the system.
- The adsorption of Pb(II) depend upon the nature of the adsorbent surface and the species distribution of Pb(II) in solution, which mainly depends on the pH of the system. The adsorption isotherm studies indicate that the adsorption of Pb(II) follows both Langmuir and Freundlich isotherms. The values of the adsorption coefficients indicate the favorable nature of adsorption of Pb(II) on the metal oxide-coated bentonites. From the values of Langmuir monolayer capacity, q_m, it is concluded that the treatment with metal oxides does increase the number of adsorption sites to a large extent. This improvement in bentonite performance may be attributed to an increase in surface charge due to the formation of magnesium oxides on the bentonite surface. The treatment also influences the strength of the existing sites as revealed by the adsorption equilibrium constant (K_L) data.
- The endothermic nature of the processes can be explained by the partial dehydration of Pb(II) before its adsorption on the bentonite samples.
- The findings require confirmation by direct methods such as extended X-ray absorption fine structure (EXAFS).

References

[1] S. Veli, B. Alyüz, Adsorption of copper and zinc from aqueous solutions by using natural clay, Journal of Hazardous Materials 149 (2007) 226–233.
[2] G.A. Castro, M.G. Echegarrua, M.A. Perez, R. Moreno-Tost, E. Rodrıguez-Castellon, A. Jimenez-Lopez, Adsorption properties of natural and Cu(II), Zn(II), Ag(I) exchanged cuban mordenites, Microporous and Mesoporous Materials 108 (2008) 325–332.
[3] D. Karamanis, P.A. Assimakopoulos, Efficiency of aluminum-pillared montmorillonite on the removal of cesium and copper from aqueous solutions, Water Research 41 (2007) 1897–1906.
[4] O. Khazali, R. Abu-El-Halawa, K. Al-Sou'od, Removal of copper(II) from aqueous solution by Jordanian pottery materials, Journal of Hazardous Materials B139 (2007) 67–71.
[5] C.L. Peacock, D.M. Sherman, Surface complexation model for multisite adsorption of copper(II) onto kaolinite, Geochimica et Cosmochimica Acta 69 (2005) 3733–3745.
[6] M. Kazemipour, M. Ansari, S. Tajrobehkar, M. Majdzadeh, H.R. Kermani, Removal of lead, cadmium, zinc, and copper from industrial wastewater by carbon developed from walnut, hazelnut, almond, pistachio shell, and apricot stone, Journal of Hazardous Materials 150 (2008) 322–327.
[7] S. Larous, A.-H. Meniai, M.B. Lehocine, Experimental study of the removal of copper from aqueous solutions by adsorption using sawdust, Desalination 185 (2005) 483–490.
[8] A. Hammaini, F. Gonzalez, A. Ballester, M.L. Blazquez, J.A. Munoz, Simultaneous uptake of metals by activated sludge, Minerals Engineering 16 (2003) 723–729.
[9] S. Lu, S.W. Gibb, Copper removal from wastewater using spent-grain as biosorbent, Bioresource Technology Bioresource Technology 99 (2008) 1509–1517.

[10] B.M.W.P.K. Amarasinghe, R.A. Williams, Tea waste as a low cost adsorbent for the removal of Cu and Pb from wastewater, Chemical Engineering Journal 132 (2007) 299–309.
[11] Y.-H. Huang, C.-L. Hsueh, H.-P. Cheng, L.-C. Su, C.-Y. Chen, Thermodynamics and kinetics of adsorption of Cu(II) onto waste iron oxide, Journal of Hazardous Materials 144 (2007) 406–411.
[12] A. Papandreou, C.J. Stournaras, D. Panias, Copper and cadmium adsorption on pellets made from fired coal fly ash, Journal of Hazardous Materials 148 (2007) 538–547.
[13] I.J. Alinnor, Adsorption of heavy metal ions from aqueous solution by fly ash, Fuel 86 (2007) 853–857.
[14] P.F. Luckham, S. Rossi, The colloidal and rheological properties of bentonite suspensions, Advances Colloid Interfaces Science 82 (1999) 43–92.
[15] E. Eren, Removal of copper ions by modified Unye clay, Turkey, Journal of Hazardous Materials 159 (2008) 235–244.
[16] B.D. Lee, M.R. Walton, J.L. Megio, Biological and chemical interactions with U(VI) during anaerobic enrichment in the presence of iron oxide coated quartz, Water Research 39 (2005) 4363–4374.
[17] Y. Xu, L. Axe, Synthesis and characterization of iron oxide-coated silica and its effect on metal adsorption, Journal of Colloid and Interface Science 282 (2005) 11–19.
[18] R. Han, W. Zoua, Z. Zhang, J. Shi, J. Yang, Removal of copper(II) and lead(II) from aqueous solution by manganese oxide coated sand I. Characterization and kinetic study, Journal of Hazardous Materials B137 (2006) 384–395.
[19] R. Han, W. Zou, H. Li, Y. Li, J. Shi, Copper(II) and lead(II) removal from aqueous solution in fixed-bed columns by manganese oxide coated zeolite, Journal of Hazardous Materials 137 (2006) 934–942.
[20] W. Zou, R. Han, Z. Chen, Z. Jinghua, J. Shi, Kinetic study of adsorption of Cu(II) and Pb(II) from aqueous solutions using manganese oxide coated zeolite in batch mode, Colloids and Surfaces A: Physicochemical Engineering Aspects 279 (2006) 238–246.
[21] E. Eren, B. Afsin, Y. Onal, Removal of lead ions by acid activated and manganese oxide-coated bentonite, Journal of Hazardous Materials 161 (2009) 677–685.
[22] R. Dohrmann, Cation exchange capacity methodology I: an efficient model for the detection of incorrect cation exchange capacity and exchangeable cation results, Applied Clay Science 34 (2006) 31–37.
[23] A. Dimirkou, M.K. Doula, Use of clinoptilolite and an Fe-overexchanged clinoptilolite in Zn^{2+} and Mn^{2+} removal from drinking water, Desalination 224 (2008) 280–292.
[24] C.H. Lai, C.Y. Chen, Removal of metal ions and humic acid from water by iron-coated filter media, Chemosphere 44 (2001) 1177–1184.
[25] N-A.M. Deraz, Physicochemical properties and catalytic behavior of magnesia supported manganese oxide catalysts, Thermochimica Acta 421 (2004) 171–177.
[26] I.F. Mironyuk, V.M. Gunko, M.O. Povazhnyak, V.I. Zarko, V.M. Chelyadin, R. Leboda, J. Skubiszewska-Zieba, W. Janusz, Magnesia formed on calcination of $Mg(OH)_2$ prepared from natural bischofite, Applied Surface Science 252 (2006) 4071–4082.
[27] I. Langmuir, The adsorption of gases on plane surfaces of glass, mica and platinum, Journal of the American Society 40 (1918) 1361–1403.
[28] H. Freundlich, Über die adsorption in lösungen, Zeitschrift für Physikalische Chemie (Leipzig) 57 (1906) 385–470.
[29] A. Sarı, M. Tuzen, M. Soylak, Adsorption of Pb(II) and Cr(III) from aqueous solution on Celtek clay, Journal of Hazardous Materials 144 (2007) 41–46.
[30] A. Sarı, M. Tuzen, D. Cıtak, M. Soylak, Adsorption characteristics of Cu(II) and Pb(II) onto expanded perlite from aqueous solution, Journal of Hazardous Materials 148 (2007) 387–394.
[31] D. Xu, X.L. Tan, C.L. Chen, X.K. Wang, Adsorption of Pb(II) from aqueous solution to MX-80 bentonite: effect of pH, ionic strength, foreign ions and temperature, Applied Clay Science 41 (2008) 37–46.
[32] A. Gunay, E. Arslankaya, I. Tosun, Lead removal from aqueous solution by natural and pretreated clinoptilolite: Adsorption equilibrium and kinetics, Journal of Hazardous Materials 146 (2007) 362–371.
[33] K.G. Bhattacharyya, S.S. Gupta, Adsorption of Fe(III) from water by natural and acid activated clays: studies on equilibrium isotherm, kinetics and thermodynamics of interactions, Adsorption 12 (2006) 185–204.
[34] G. Szöllösi, A. Mastalir, M. Bartok, Effect of ion exchange by an organic cation on platinum immobilization on clays, Reaction Kinetics and Catalysis Letters 74 (2001) 241–249.
[35] S. Zhu, H. Hou, Y. Xue, Kinetic and isothermal studies of lead ion adsorption onto bentonite, Applied Clay Science 40 (2008) 171–178.
[36] S.S. Gupta, K.G. Bhattacharyya, Immobilization of Pb(II), Cd(II) and Ni(II) ions on kaolinite and montmorillonite surfaces from aqueous medium, Journal of Environmental Management 87 (2008) 46–58.
[37] K.G. Bhattacharyya, S.S. Gupta, Adsorptive accumulation of Cd(II), Co(II), Cu(II), Pb(II), and Ni(II) from water on montmorillonite: Influence of acid activation, Journal of Colloid Interface Science 310 (2007) 411–424.
[38] A. Gunay, E. Arslankaya, I. Tosun, Lead removal from aqueous solution by natural and pretreated clinoptilolite: adsorption equilibrium and kinetics, Journal of Hazardous Materials 146 (2007) 362–371.
[39] Y.S. Al-Degs, M.I. El-Barghouthi, A.A. Issa, M.A. Khraisheh, G.M. Walker, Sorption of Zn(II), Pb(II), and Co(II) using natural sorbents: equilibrium and kinetic studies, Water Research 40 (2006) 2645–2658.
[40] A. Ozer, Removal of Pb(II) ions from aqueous solutions by sulphuric acid-treated wheat bran, Journal of Hazardous Materials 141 (2007) 753–761.
[41] A. Sari, M. Tuzen, D. Citak, M. Soylak, Equilibrium, kinetic and thermodynamic studies of adsorption of Pb(II) from aqueous solution onto Turkish kaolinite clay, Journal of Hazardous Materials 149 (2007) 283–291.
[42] A. Kaya, S. Durukan, Utilization of bentonite-embedded zeolite as clay liner, Applied Clay Science 25 (2004) 83–91.
[43] S. Yin, Z. Jiang, G. Chang, B. Hu, Simultaneous on-line preconcentration and determination of trace metals in environmental samples by flow injection combined with inductively coupled plasma mass spectrometry using a nanometer-sized alumina packed micro-column, Analytica Chimica Acta 540 (2005) 333–339.
[44] R. Han, Z. Lu, W. Zou, W. Daotong, J. Shi, Y. Jiujun, Removal of copper(II) and lead(II) from aqueous solution by manganese oxide coated sand: II. Equilibrium study and competitive adsorption, Journal of Hazardous Materials 137 (2006) 480–488.
[45] Y.-H. Huang, C.-L. Hsueh, C.-P. Huang, L.-C. Su, C.-Y. Chen, Adsorption thermodynamic and kinetic studies of Pb(II) removal from water onto a versatile Al_2O_3-supported iron oxide, Separation and Purification Technology 55 (2007) 23–29.
[46] Y. Al-Degs, M.A.M. Khraisheh, M.F. Tutunji, Sorption of lead ions on diatomite and manganese oxides modified diatomite, Water Research 35 (2001) 3724–3728.
[47] S.-G. Wang, W.-X. Gong, X.-W. Liu, Y.-W. Yao, B.-Y. Gao, Q.-Y. Yue, Removal of lead(II) from aqueous solution by adsorption onto manganese oxide-coated carbon nanotubes, Separation and Purification Technology 58 (2007) 17–23.
[48] C.-H. Weng, C.-Z. Tsai, S.-H. Chu, Y.C. Sharma, Adsorption characteristics of copper(II) onto spent activated clay, Separation and Purification Technology 54 (2007) 187–197.
[49] L.M. Nunes, C. Airoldi, Some features of crystalline α-titanium hydrogen phosphate, modified sodium and *n*-butylammonium forms and thermodynamics of ionic exchange with K^+ and Ca^{2+}, Thermochimica Acta 328 (1999) 297–305.
[50] E. Eren, B. Afsin, An investigation of Cu(II) adsorption by raw and acid-activated bentonite: a combined potentiometric, thermodynamic, XRD, IR, DTA study, Journal of Hazardous Materials 151 (2008) 682–691.
[51] R. Naseem, S.S. Tahir, Removal of Pb(II) from aqueous/acidic solutions by using bentonite as an adsorbent, Water Research 35 (2001) 3982–3986.
[52] R. Donat, A. Akdogan, E. Erdem, H. Cetisli, Thermodynamics of Pb^{2+} and Ni^{2+} adsorption onto natural bentonite from aqueous solutions, Journal of Colloid and Interface Science 286 (2005) 43–52.
[53] P.J. Pretorius, P.W. Linder, The adsorption characteristics of δ-manganese dioxide: a collection of diffuse double layer constants for the adsorption of H^+, Cu^{2+}, Ni^{2+}, Zn^{2+}, Cd^{2+} and Pb^{2+}, Applied Geochemistry 16 (2001) 1067–1082.
[54] M. Park, C.L. Choi, Y.J. Seo, S.K. Yeo, J. Choi, S. Komarneni, J.H. Lee, Reactions of Cu^{2+} and Pb^{2+} with Mg/Al layered double hydroxide, Applied Clay Science 37 (2007) 143–148.
[55] Y. Xu, T. Boonfueng, L. Axe, S. Maeng, T. Tyson, Surface complexation of Pb(II) on amorphous iron oxide and manganese oxide: spectroscopic and time studies, Journal of Colloid and Interface Science 299 (2006) 28–40.